Spin-Exchange-Pumped ^{3}He and ^{129}Xe Zeeman Masers

T. E. Chupp,[2] R. J. Hoare,[1] R. L. Walsworth,[3] and Bo Wu[2]

[1]*Harvard University, Cambridge, Massachusetts 02138*

[2]*University of Michigan, Ann Arbor, Michigan 48109*

[3]*Smithsonian Astrophysical Observatory, Cambridge, Massachusetts 02138*

(Received 15 November 1993)

Steady-state noble gas Zeeman masers operating with ^{3}He and ^{129}Xe have been realized by spin exchange with laser optically pumped Rb. These masers can operate continuously for arbitrary lengths of time. For measurement intervals $\tau = 1000$ to 10000 s, frequency measurement precision for a phase locked ^{129}Xe maser is shown to be better than $1\times10^{-2}\tau^{-3/2}$ Hz. Startup transients are used to study gain characteristics. In a two-cell setup maser conditions for both species can be optimized allowing a wide array of precision measurements.

PACS numbers: 32.80.Bx, 42.52.+x

Precision measurement of the Zeeman splitting in a two-state system is the basis of the traditional magnetometer (e.g., proton NMR [1]), optically pumped atomic magnetometers [2], as well as searches for exotic nonmagnetic couplings such as the permanent electric dipole moment (EDM) of the neutron [3] or atoms [4–8]. Previous work demonstrated a Zeeman maser operating with ^{3}He polarized by optical pumping of metastable atoms [9,10]. We report here the successful operation of a new system: the spin-exchange-pumped noble gas Zeeman maser in which the population inversion is produced by spin exchange between the noble gas and optically pumped Rb vapor.

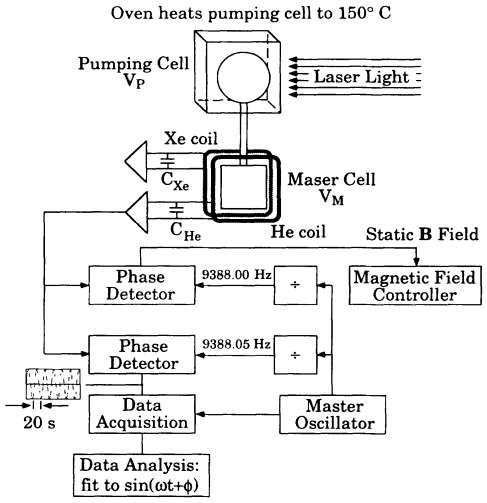

FIG. 1. The noble gas Zeeman maser apparatus. The two-cell system necessary for dual species operation is illustrated. For the experimental results presented in this paper, we used a single cell in the measurement cell position. The laser optically pumps Rb atoms that transfer spin to the noble gas nuclei. Each pickup coil is part of a tank circuit tuned to the noble gas precession frequency. The magnetic energy stored in the tank circuit is oscillating at the precession frequency and causes Rabi precession, which rotates the spins toward the lower energy state.

Our goal is a dual species maser with ^{3}He and ^{129}Xe. Dual species operation is important for experiments that measure frequency shifts due to new physics such as the existence of an atomic EDM, which would be several orders of magnitude smaller for ^{3}He than for ^{129}Xe [8,11]. Spin exchange can simultaneously produce polarization of more than one noble gas species [11], and dual maser operation can be effected in a two-cell system, in which conditions for both species can be optimized. (Dual species operation is difficult in a single cell, because threshold and optimum conditions for each species are different and competing.) To date, we have achieved continuous maser operation separately with ^{3}He and ^{129}Xe in a single cell and with ^{3}He in a two-cell system.

We begin with the formalism and description of the two-cell system necessary for the dual species Zeeman maser. A pumping cell (labeled V_P) and a measurement or maser cell (labeled V_M) are connected by a transfer tube [12] (see Fig. 1). Maser oscillation is effected by the coupling of precessing spins to a resonant cavity or, in our case, a tank circuit formed by the pickup coil and a tuning capacitor (see Fig. 1). The precessing magnetization induces a current and therefore a resonant oscillating magnetic field, which produces a torque on the spins that changes the magnetization. This self-coupling can lead to stimulated or super-radiant Rabi precession of the spins and, if a continuous source of magnetization is present, to steady-state maser oscillations with stable longitudinal and transverse magnetizations. Spin exchange in the pumping cell provides the continuous source of magnetization as the longitudinally polarized atoms diffuse into the maser cell. Spins in the pumping cell do not take part in the maser oscillation because the transverse component of magnetization in the pumping cell is rapidly damped by spin exchange and by the magnetic field gradients.

The equations of motion for the spins of each species in the Zeeman maser can be written as modified Bloch equations combined with source terms due to spin exchange and transfer of polarization from the pumping cell to maser cell [10,12]:

0031-9007/94/72(15)/2363(4)$06.00

$$\dot{P}_x = (P_y\omega_z - P_z\omega_y) - \frac{P_x}{T_2},$$

$$\dot{P}_y = (P_z\omega_x - P_x\omega_z) - \frac{P_y}{T_2},$$

$$\dot{P}_z = (P_x\omega_y - P_y\omega_x) - \frac{P_z}{T_1} + (P_P - P_z)G_M,$$

$$\dot{P}_P = (P_{Rb} - P_P)\gamma_{SE} - \frac{P_P}{T_1} - (P_P - P_z)G_P, \quad (1)$$

where the polarization in the maser cell, $\mathbf{P}$, is defined by $\mathbf{M}_{ng} = \mathbf{P}_{ng}\mu_{ng}[n]$, $\mathbf{M}_{ng}$ is the magnetization (magnetic moment density), μ_{ng} is the magnetic moment, and $[n]$ is the number density of the noble gas species. P_P is the longitudinal (i.e., z component) of the noble gas polarization in the pumping cell. The vector $\boldsymbol{\omega} = \gamma_{ng}\mathbf{B}$, where γ_{ng} is the gyromagnetic ratio of the noble gas species and $\mathbf{B}$ is the sum of the static and induced oscillating magnetic fields. T_1 is the phenomenological relaxation time for longitudinal polarization (P_z and P_P) and T_2 is that for transverse polarization in the maser cell (P_x and P_y), which is affected most strongly by magnetic field gradients and spin transfer between the maser cell and pumping cell. The polarization of the laser optically pumped Rb is P_{Rb}, and γ_{SE} is the noble gas Rb spin exchange rate. G_P and G_M are polarization transfer rates out of the pumping cell and into the maser cell [12]. In Eq. (1) we assume that a conserved current of atoms in each spin state flows from one cell to the other, which requires that polarization relaxation in the transfer tube is negligible.

Transverse components of $\boldsymbol{\omega}$ are due to the current in the pickup coil induced by the precessing spins. The magnitude of the current is $I = \rho(\omega_z)\omega_z\Phi/R$, where $\Phi = \mu_0 M_T \eta A$ is the flux coupled from the transverse components of magnetization ($M_T = \sqrt{M_x^2 + M_y^2}$) to the pickup coil of area A and resistance R, and η is a geometric factor that accounts for the difference in volume of the pickup coil and the magnetized sample. $\rho(\omega_z/\omega_0)$ is the response of the pickup coil circuit:

$$\rho\left(\frac{\omega_z}{\omega_0}\right) = \frac{Q}{\sqrt{(\omega_z/\omega_0)^2 + Q^2(\omega_z/\omega_0 - 1)^2}},$$

where $Q = \omega_0 L/R$ is the quality factor of the pickup coil tank circuit, and ω_0 is the coil resonant frequency.

It is convenient to transform to a frame corotating with the precessing spins around the z axis. In this frame the magnetization is directed along the x axis. Neglecting the high frequency (e.g., Bloch-Siegert) components of the magnetic field in the rotating frame we have $\omega_z = 0$, and

$$\omega_x = \tfrac{1}{2}\gamma_{ng}\eta(\omega_z/\omega_0)\rho(\omega_z/\omega_0)\mu_0 M_T \sin\phi,$$

$$\omega_y = -\tfrac{1}{2}\gamma_{ng}\eta(\omega_z/\omega_0)\rho(\omega_z/\omega_0)\mu_0 M_T \cos\phi, \quad (2)$$

where ϕ is the phase angle between the voltage and current in the pickup coil circuit: $\tan\phi = Q(\omega_z^2 - \omega_0^2)/\omega_z\omega_0$. In the rotating frame, with $\phi = 0$, the time dependence of polarization in the maser cell can be written

$$\dot{P}_x = P_x\left(\frac{P_z}{P_0\tau_{RD}} - \frac{1}{T_2}\right),$$

$$\dot{P}_z = P_P G_M - \frac{P_x^2}{P_0\tau_{RD}} - P_z\left(\frac{1}{T_1} + G_M\right), \quad (3)$$

where $1/\tau_{RD}$, often called the radiation damping rate, is a measure of the torque that is self-induced by the spin-coil coupling,

$$\frac{1}{\tau_{RD}} = \frac{1}{2}\gamma_{ng}^2\eta Q\mu_0\frac{\hbar}{2}[n]P_0, \quad (4)$$

P_0 is the equilibrium value of P_z in the absence of spin-cavity coupling (i.e., $\tau_{RD} \to \infty$), and $P_z \le P_0$. For a single cell maser, Eqs. (3) can be modified by setting $P_P = P_{Rb}$ and $G_M = \gamma_{SE}$. The solution of these coupled equations depends on initial conditions. The conditions for steady-state maser oscillation, found by setting $\dot{P}_x = \dot{P}_z = \dot{P}_P = 0$, are (1) $P_z > 0$ (i.e., population inversion), (2) $\tau_{RD} < T_2$, and (3) $P_x > 0$. The last condition (3) is required for the maser to start and can be induced by spontaneous emission, blackbody radiation, or with a pulse of applied oscillating magnetic field [10].

In Fig. 2 we show the results of a calculation for a single-cell maser with conditions similar to those for the single-cell ^{129}Xe maser described below. The calculation shows components of polarization for maser startup from the condition $P_z = 0$ and a small transverse polarization "seed" of $P_x = 0.001$. The illustrated transient behavior can be understood as follows: Spin exchange produces polarization P_z, which builds up and increases the radiation damping torque. When that torque exceeds the threshold defined by $\tau_{RD} < (P_z/P_0)T_2$, P_x can increase as the polarization rotates. Thus P_z decreases, decreasing the radiation damping torque until a temporary equilibrium is attained from which the process repeats. Eventually, the transients decay, and steady-state oscillation proceeds.

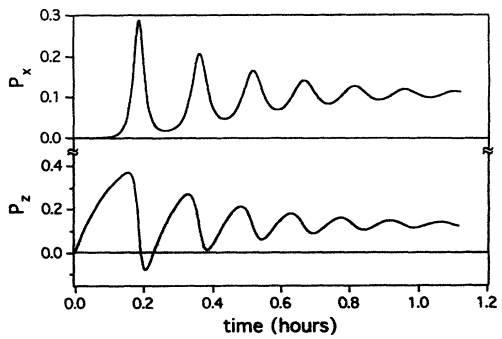

FIG. 2. Calculations of startup transients and approach to steady state for the single-cell ^{129}Xe maser with conditions similar to those listed in Table I.

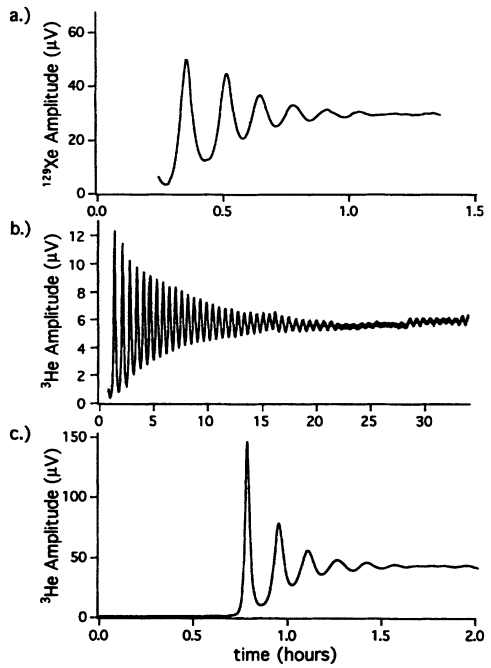

FIG. 3. Observed startup transients and approach to steady state for the single-cell ^{129}Xe (a) and the ^{3}He (b) masers and the two-cell ^{3}He maser (c). At time $t \approx 0$, $\mathbf{P} = 0$ and optical pumping was started. For the data in panel (c), the phase locked loop was closed at $t \approx 0.65$ h.

In Fig. 3 we show the measured maser signal (proportional to M_T) for the startup and approach to the steady state of separate single-cell masers using ^{129}Xe (a) and ^{3}He (b) and for a two-cell ^{3}He maser (c). The single cell is spherical in shape with volume approximately 1 cm^3 and is coated with a siliconizing agent which increases the wall relaxation time for ^{129}Xe [8]. The double cells, each spherical with volume ≈ 3 cm^3 are uncoated. The relevant parameters are given in Table I. In particular, note that the coherence relaxation times T_2 are short compared to previously observed free induction decay times of 1000 s or more [11]. For the single-cell maser, this is due to spin exchange with the polarized Rb which affects both species but is much stronger for ^{129}Xe [13]. In the two-cell maser the Rb density is much less in the lower temperature maser cell and the spin exchange effects on T_2 for ^{129}Xe will be negligible. In our current two-cell setup, the maser cell is in a region of strong magnetic field gradients which leads to the short T_2 for ^{3}He. Also note that the ^{3}He gyromagnetic ratio is 2.76 times larger than that of ^{129}Xe, which makes ω_z and Q correspondingly larger and τ_{RD} significantly smaller so that the maser threshold can be attained with smaller P_z. For the single-cell maser, the rate at which the transients damp out is determined by γ_{SE}. For the two-cell ^{3}He maser, the transients damp out with a rate characteristic of the spin transfer rate $G_M \approx 1/(3 \text{ min})$.

The utility of the noble gas maser for magnetometry and searches for exotic dipole couplings (e.g., a permanent EDM of ^{129}Xe) is illustrated in an experiment that uses the maser precession frequency to lock the magnetic field while monitoring the maser oscillation frequency. In this experiment, the maser serves as a phase locked local oscillator which is compared to a master clock as shown in Fig. 1. This measurement is not sensitive to the intrinsic frequency stability of the maser for observation times long compared to the time constants of the phase locked loop, and it therefore establishes the limits of the maser frequency precision. The frequency was measured by beating the maser signals against a reference oscillator shifted from the lock frequency by 0.05 Hz (i.e., for the single-cell ^{3}He maser, the reference oscillator is at 9388.05 Hz). This beat signal was averaged with a 1.25 s time constant and sampled at 1 Hz.

The measured frequency is defined as the best fit frequency extracted from a χ^2 minimization of the data stream, which can be thought of as a linear fit of the phase as a function of time. In our case, the phase is determined by the measured signal voltage with the relationship $v(t_i) = v_0 \sin[\phi(t_i)]$, where v_0 is the amplitude of the measured voltage. The expected optimal maser frequency performance, the precision for a given measurement interval τ, is limited by the error on the slope of ϕ as a function of time. For our measurements, with τ between 1000 and 10000 s, this is dominated by the white voltage noise from the pickup coil at temperature T and noise from the electronics which cause white phase noise

TABLE I. Noble gas Zeeman maser parameters.

	^{129}Xe	^{3}He (single cell)	^{3}He (double cell)
Operating temperature	80 °C	150 °C	150 °C (pump)/90 °C (maser)
[Rb]	1.4×10^{12}/cm^3	1.0×10^{14}/cm^3	1.0×10^{14}/cm^3
$[n]$	7×10^{18}/cm^3	1.4×10^{19}/cm^3	4.9×10^{19}/cm^3
γ_{SE}^{-1}	0.2 h	22 h	22 h
P_0	≈ 1	< 0.2	≈ 0.3
Q	13	30	10
τ_{RD}	≈ 25 s	> 2 s	1.5 s
T_2	100 s	180 s	12 s
Signal size (v_0)	30 μV	6 μV	40 μV
Operating frequency	3510 Hz	9388 Hz	9760 Hz

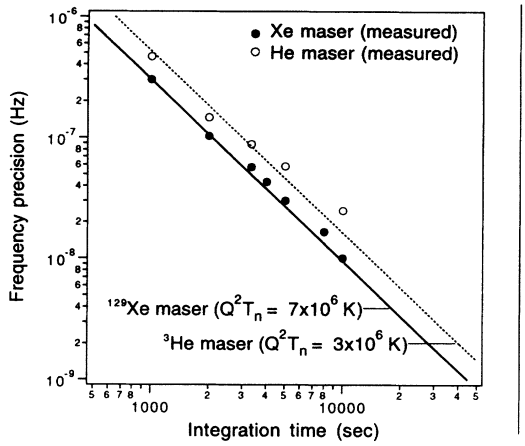

FIG. 4. Frequency precision of the single-cell ^{3}He and ^{129}Xe masers. In both cases, the maser oscillation frequency is locked to an external oscillator by feedback to the static magnetic field. The maser serves as a local oscillator that is compared to the reference frequency for variable integration times, τ. The solid and dashed lines are proportional to $\tau^{-3/2}$, which is expected for limitations due solely to white phase noise.

of uniform density given by

$$\phi_{\rm rms}^2/B \approx 4kR(Q^2T + T_{\rm amp} + \cdots)/v_0^2 , \quad (5)$$

where B is the bandwidth of the electronics. Fluctuations of the maser frequency on time scales short compared to the 0.05 Hz beat frequency also appear as phase noise and cannot be separated from the voltage noise. For white phase noise, the error on the measured frequency can be shown to be [14]

$$\sigma_\nu = \frac{1}{2\pi}\left(\frac{12}{\pi}\frac{\phi_{\rm rms}^2/B}{\tau^3}\right)^{1/2} \propto \tau^{-3/2} , \quad (6)$$

where we assume that B is matched to the sample rate so that the number of samples is $N = 2\pi B\tau$. The intrinsic frequency noise of the maser includes unstable collisional and wall induced shifts and imperfect operation of the magnetic field lock loop. White frequency noise causes a random walk of the phase that accumulates as $\phi_{\rm rms}^2 \propto \tau$ [15], and for τ sufficiently large so that white frequency noise dominates, we would expect $\sigma_\nu \propto \tau^{-1/2}$ [16].

In Fig. 4 we show the results of our measurements for the single-cell ^{3}He and ^{129}Xe masers. Each data point represents the standard deviation of a series of measurements for each measurement interval τ. The data demonstrate that $\sigma_\nu \propto \tau^{-3/2}$ (solid and dashed lines) as expected for the phase locked maser. We can extract the effective noise temperature ($Q^2T_{\rm eff} = Q^2T + T_{\rm amp} + \cdots$) and find $Q^2T_{\rm eff} = 3\times10^6$ K for ^{3}He and $Q^2T_{\rm eff} = 7\times10^6$ K for ^{129}Xe. For the ^{3}He maser pickup coil $Q^2T = 4\times10^5$ K, and for the ^{129}Xe maser $Q^2T = 6\times10^4$ K. This shows that voltage and phase noise are 4 and 10 times greater, respectively, than that due to pickup coil Johnson noise alone.

In summary, we have demonstrated successful operation of versatile spin-exchange-pumped noble gas Zeeman masers that are appropriate for precision magnetometry and, when operating with two or more species, searches for exotic dipole couplings. The performance achieved to date for the single-cell, single species, phase locked ^{129}Xe maser can be expressed as $\sigma_\nu < 10^{-2}\tau^{-3/2}$ Hz for measurement intervals $\tau = -1000$ to 10000 s. We anticipate significant improvement of this performance in the optimized two-cell configuration (increasing v_0 and utilizing optimized pickup coil geometry). Also note that, since maser performance is dominated by pickup coil Johnson noise and other sources of white voltage noise, a dc SQUID detecting the precessing magnetization could also lead to improved performance. Operation with other noble gas species, including ^{21}Ne, is straightforward, providing opportunities for a wide array of applications.

The authors are grateful for the efforts of and discussions with Mark Wagshul, Eduardo Oteiza, Miriam Vu, Reginald Jaynes, Edward Mattison, and Robert Vessot. This work was supported by the University of Michigan and the Smithsonian Institution's Scholary Studies Program.

[1] A. Abragham, *Principle of Magnetic Resonance* (Oxford Univ. Press, Oxford, 1961), p. 91.
[2] W. Farr and E. Otten, Appl. Phys. **3**, 367 (1974).
[3] K. F. Smith *et al.*, Phys. Lett. B **234**, 191 (1990).
[4] J. P. Jacobs, W. M. Klipstein, S. K. Lamoreaux, B. R. Heckel, and E. N. Fortson, Phys. Rev. Lett. **71**, 3782 (1993).
[5] S. A. Murthy, D. Krause, Z. Li, and L. R. Hunter, Phys. Rev. Lett. **63**, 965 (1989).
[6] K. Abdullah, C. Carlberg, E. D. Commins, H. Gould, and S. Ross, Phys. Rev. Lett. **65**, 2347 (1990).
[7] D. Cho, K. Sangster, and E. A. Hinds, Phys. Rev. Lett. **63**, 2559 (1989).
[8] E. R. Oteiza, Ph.D. dissertation, Harvard University (1992); T. E. Chupp *et al.*, in *The Search for a Permanent Electric Dipole Moment using ^{129}Xe and ^{3}He*, AIP Conf. Proc. No. 270 (AIP, New York, 1993), p. 84; R. J. Hoare *et al.*, in *Atomic Physics 13*, AIP Conf. Proc. No. 275 (AIP, New York, 1993), p. 73.
[9] H. G. Robinson and T. Myint, Appl. Phys. Lett. **5**, 116 (1964).
[10] M. G. Richards, B. P. Cwan, M. F. Secca, and K. Machin, J. Phys. B **21**, 665 (1988).
[11] T. E. Chupp, E. R. Oteiza, J. M. Richardson, and T. R. White, Phys. Rev. A **38**, 3998 (1988); T. E. Chupp and R. J. Hoare, Phys. Rev. Lett. **64**, 2261 (1990).
[12] T. E. Chupp, R. A. Loveman, A. K. Thompson, A. M. Bernstein, and D. R. Tieger, Phys. Rev. C **45**, 915 (1992).
[13] X. Zeng *et al.*, Phys. Rev. A **31**, 260 (1985).
[14] T. E. Chupp, R. J. Hoare, R. L. Walsworth, and B. Wu (to be published).
[15] D. W. Allen, Proc. IEEE **54**, 221 (1966).
[16] R. F. C. Vessot, L. Mueller, and J. Vanier, Proc. IEEE **54**, 199 (1966).

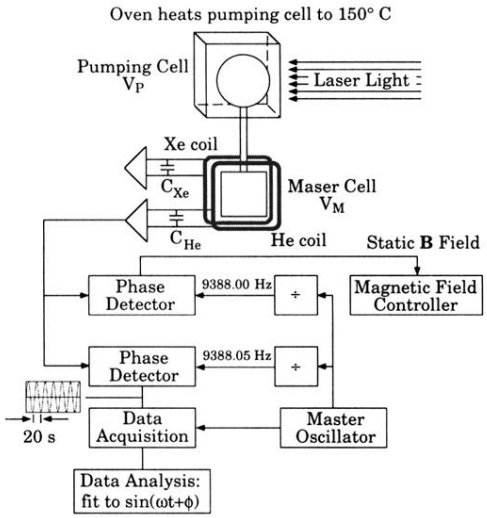

FIG. 1. The noble gas Zeeman maser apparatus. The two-cell system necessary for dual species operation is illustrated. For the experimental results presented in this paper, we used a single cell in the measurement cell position. The laser optically pumps Rb atoms that transfer spin to the noble gas nuclei. Each pickup coil is part of a tank circuit tuned to the noble gas precession frequency. The magnetic energy stored in the tank circuit is oscillating at the precession frequency and causes Rabi precession, which rotates the spins toward the lower energy state.